BJP British Journal of Pharmacology

DOI:10.1111/bph.13193
www.brjpharmacol.org

RESEARCH PAPER

Prevention of the degeneration of human dopaminergic neurons in an astrocyte co-culture system allowing endogenous drug metabolism

Liudmila Efremova[1,2], Stefan Schildknecht[1], Martina Adam[1], Regina Pape[1], Simon Gutbier[1,2], Benjamin Hanf[2,3], Alexander Bürkle[3] and Marcel Leist[1]

[1]*Doerenkamp-Zbinden Chair for In Vitro Toxicology and Biomedicine,* [2]*Research Training Group 1331 (RTG1331),* [3]*Molecular Toxicology Group, University of Konstanz, Konstanz, Germany*

Correspondence
Marcel Leist,
Doerenkamp-Zbinden Chair for In Vitro Toxicology and Biomedicine, University of Konstanz, PO Box M657, D-78457 Konstanz, Germany.
E-mail:
Marcel.Leist@uni-konstanz.de

Received
7 October 2014
Revised
4 May 2015
Accepted
12 May 2015

BACKGROUND AND PURPOSE

Few neuropharmacological model systems use human neurons. Moreover, available test systems rarely reflect functional roles of co-cultured glial cells. There is no human *in vitro* counterpart of the widely used 1-methyl-4-phenyl-tetrahydropyridine (MPTP) mouse model of Parkinson's disease

EXPERIMENTAL APPROACH

We generated such a model by growing an intricate network of human dopaminergic neurons on a dense layer of astrocytes. In these co-cultures, MPTP was metabolized to 1-methyl-4-phenyl-pyridinium (MPP^+) by the glial cells, and the toxic metabolite was taken up through the dopamine transporter into neurons. Cell viability was measured biochemically and by quantitative neurite imaging, siRNA techniques were also used.

KEY RESULTS

We initially characterized the activation of PARP. As in mouse models, MPTP exposure induced (poly-ADP-ribose) synthesis and neurodegeneration was blocked by PARP inhibitors. Several different putative neuroprotectants were then compared in mono-cultures and co-cultures. Rho kinase inhibitors worked in both models; CEP1347, ascorbic acid or a caspase inhibitor protected mono-cultures from MPP^+ toxicity, but did not protect co-cultures, when used alone or in combination. Application of GSSG prevented degeneration in co-cultures, but not in mono-cultures. The surprisingly different pharmacological profiles of the models suggest that the presence of glial cells, and the *in situ* generation of the toxic metabolite MPP^+ within the layered cultures played an important role in neuroprotection.

CONCLUSIONS AND IMPLICATIONS

Our new model system is a closer model of human brain tissue than conventional cultures. Its use for screening of candidate neuroprotectants may increase the predictiveness of a test battery.

Abbreviations

CEP1347, (3,9-bis[(ethylthio)methyl]-K-252a); DAT, dopamine transporter; DHQ, 1,5- isoquinolinediol; DM, differentiation medium; DTNB, 5,5′-dithiobis(2-nitrobenzoic acid); IMA, immortalized mouse astrocytes; MPP^+, 1-methyl-4-phenyl-pyridinium; MPTP, 1-methyl-4-phenyl-1,2,3,6-tetrahydropyridine; PD, Parkinson's disease; ROCK, Rho kinase

Tables of Links

TARGETS
Transporters[a]
DAT, dopamine transporter
Vesicular monoamine transporter (VMAT2; SLC 18A2)
Enzymes[b]
MAO-B, monoamine oxidase B
Mixed lineage kinase MLK1
NOS, nitric oxide synthase
TH, tyrosine hydroxylase
PARP, poly (ADP-ribose) polymerase

LIGANDS	
1400W	MPP+, 1-methyl-4-phenyl-pyridinium.
7-Nitroindazole	NO
ABT-888, veliparib	Rasagiline,
Ascorbic acid	Y-27632
CEP-1347	
Deprenyl (selegiline)	
Dopamine	
GSH	
HA-1077, fasudil	

These Tables list key protein targets and ligands in this article which are hyperlinked to corresponding entries in http://www.guidetopharmacology.org, the common portal for data from the IUPHAR/BPS Guide to PHARMACOLOGY (Pawson *et al.*, 2014) and are permanently archived in the Concise Guide to PHARMACOLOGY 2013/14 ([a,b]Alexander *et al.*, 2013a,b).

Introduction

Degeneration of dopaminergic neurons plays an important role in Parkinson's disease (PD) and there is, therefore, a great need for new models that allow testing of potential neuroprotective drugs (Schapira *et al.*, 2005; Schule *et al.*, 2009; Youdim, 2010). Although some forms of PD have a genetic background, such as mutations of α-synuclein, about 90% of disease cases have an unclear aetiology. Some of these may be caused or promoted by toxicants such as manganese, rotenone or dieldrin (Caudle *et al.*, 2012; Pan-Montojo *et al.*, 2012). Several neuroprotective drugs have been developed so far, but none of the pharmacological agents has yet been shown convincingly to slow the progression of PD (Meissner *et al.*, 2011). One major obstacle in the development of novel neuroprotective strategies and the discovery of early disease biomarkers is the limited availability of human cell-based neuronal models. Moreover, most of the available ones are lacking active neuron–glia interactions (Schule *et al.*, 2009), although astrocytes are increasingly recognized as exerting important effects on neurons. For instance, they may regulate neurite outgrowth not only during fetal development but also during regeneration from damage (Giordano and Costa, 2012).

The best studied chemical that reproducibly triggers degeneration of dopaminergic neurons is 1-methyl-4-phenyl-1,2,3,6-tetrahydropyridine (MPTP). This compound triggers toxicity in the human nigrostriatal pathway with high specificity (Langston *et al.*, 1984). MPTP itself does not adversely affect neuronal cell cultures and its toxicity is consequent on metabolic transformation to the actual toxin 1-methyl-4-phenyl-pyridinium (MPP^+). Conversion of MPTP to its toxic metabolite requires MAO activity, which is mainly found in astrocytes within the brain (Schulz *et al.*, 1995). MPP^+ is then taken up by dopaminergic neurons via their dopamine transporter (DAT).

Thus, the metabolism, distribution and neurotoxicity require complex neuron–glia interactions (Dauer and Przedborski, 2003). In most cases, MPTP toxicity is modelled *in vitro* by direct application of the active metabolite MPP^+ to cells (Leist *et al.*, 1998; Zeng *et al.*, 2006; Poltl *et al.*, 2012; Peng *et al.*, 2013; Sun *et al.*, 2013). This approach omits the influence of glia cells, and necessarily alters the concentration–time profile of MPP^+ exposure.

Many potentially neuroprotective drugs have shown robust effects in preclinical studies but failed to be effective in clinical trials (Olanow and Kordower, 2009). A typical example is the mixed lineage kinase inhibitor CEP-1347. The compound was protective in various rodent models and *in vitro* test systems, including human neurons exposed to MPP^+ (Maroney *et al.*, 1999; Falsig *et al.*, 2004b; Schildknecht *et al.*, 2009) but it failed in clinical studies due to lack of efficacy (Parkinson Study Group PI, 2007; Yacoubian and Standaert, 2009). There have been several attempts to improve cell culture-based test systems for clinical predictivity by a transition from rodent to human cells, and by incorporation of glial cells to neuronal cultures (McNaught and Jenner, 1999; Liu *et al.*, 2009). For co-culture systems, the major focus has been on microglia as the second cell type apart from neurons (McGeer and McGeer, 2008), but astrocytes have been used, for example, with motor neurons or in order to stabilize stem cell-derived neurons (Reinhardt *et al.*, 2013; Zhang *et al.*, 2013). Concerning the transition to human cells, tumour cell lines have often been used as surrogates for neurons (Zhao *et al.*, 2013; Chong *et al.*, 2014). Only recently, the broader availability of stem cells has facilitated the generation of

human neuronal cultures for the study of neurodegenerative disease (Perrier *et al.*, 2004; Schulz *et al.*, 2004; Morizane *et al.*, 2010). As the precise culture composition is difficult to control, when cells are directly generated from pluripotent stem cells, a start from intermediate stages (neural stem cells or committed precursor cells) is frequently used in drug screening and pharmacology (Scholz *et al.*, 2011; Reinhardt *et al.*, 2013).

In a related approach, we took advantage of LUHMES cells. These are conditionally immortalized mesencephalic neuronal precursors that can be differentiated to fully post-mitotic dopaminergic neurons (Lotharius *et al.*, 2005; Scholz *et al.*, 2011). These were combined with immortalized murine astrocytes that have been extensively characterized for their metabolic capacity and inflammatory competence (Schildknecht *et al.*, 2012).

This new co-culture system allowed us to model MPTP metabolism *in vitro* and to reveal differences in pharmacological activities of mechanistically diverse, experimentally neuroprotective compounds in comparison with neuronal mono-cultures exposed to MPP^+. Our data demonstrate that neurons grown in co-culture with glia show a radically different pharmacological behaviour from that of neuronal mono-cultures. Co-cultures could provide a valuable additional model in pharmacological and toxicological studies.

Methods

Cell culture

LUHMES cells are ventral mesencephalic precursor cells from a human female fetus that have been conditionally immortalized by v-myc under the control (tet-off) of tetracycline. Inactivation of the transgene and addition of differentiation factors allows a rapid and synchronized conversion of fully post-mitotic neurons with neurites of >1000 μm in length and expression of typical dopaminergic markers. Cells were cultured as described in detail earlier (Scholz *et al.*, 2011; Schildknecht *et al.*, 2013; Krug *et al.*, 2014).

Immortalized mouse astrocyte cell line (IMA 2.1) were generated and used as previously described in detail (Schildknecht *et al.*, 2012). Primary cortical astrocytes were generated from Wistar rats bred at the animal facility of the University of Konstanz, Germany. Primary glia cells were prepared from rat pups at 24 h *post partum* as described earlier (Falsig *et al.*, 2004a).

For co-culture with LUHMES neurons, IMA or mixed primary glial cells were seeded in multiwell plates (BD Falcon, Bedford, MA, USA) in DMEM supplemented with 10% FCS and 1% penicillin/streptomycin at a density of 15 000 cm^{-2}. After 24 h, LUHMES differentiation medium (DM) was added for another 2 days. Then pre-differentiated (day 2) LUHMES cells were seeded on top of astrocytes at a density of 300 000 cells per well (24-well plates) and were further differentiated for another 4 days in LUHMES DM. The density of IMA on day 6 of the culture was 195 000 cells cm^{-2}.

Cell viability assays

The resazurin assay was performed as described earlier (Falsig *et al.*, 2004a; Schildknecht *et al.*, 2009; Zimmer *et al.*, 2011). LDH activity was detected in cell culture medium (supernatant) and cell lysates separately. LDH release was expressed as $100 \times LDH_{(supernatant)}/LDH_{(supernatant)} + LDH_{(lysate)}$. For the detection of ATP levels, a commercially available ATP assay reaction mix (Sigma-Aldrich St. Louis, MO, USA), containing luciferin and luciferase, was used (Volbracht *et al.*, 1999). As the main end point to quantify neuronal viability within co-cultures, we used an imaging-based quantification of the neuronal area, essentially as described earlier (Lotharius *et al.*, 2005; Schildknecht *et al.*, 2009; Krug *et al.*, 2013). The method uses an automated microscope that automatically records images from many different fields, and uses an established algorithm to determine the respective neuronal areas of the fields. An image-supported illustration of the method (see in Supporting Information Fig. S3) and a cross-validation of the method with manual counting of cell stomata (see in Supporting Information Fig. S5) have been provided in the supplemental material.

GSH assay

Cells were washed with PBS and lysed in 250 μL of 1% sulfosalicylic acid (w/v) for 3 min. Following sonication and centrifugation at 12 000× *g* at 4°C for the removal of cell debris, supernatant was collected. Total glutathione content was determined by a DTNB [5,5′-dithiobis(2-nitrobenzoic acid)] reduction assay. Supernatants were diluted 1:5 in H_2O; 100 μL of sample was mixed with 100 μL assay mixture containing 300 μM DTNB, 1 $U \cdot mL^{-1}$ glutathione reductase, 400 μM NADPH, 1 mM EDTA in 100 mM sodium phosphate buffer, pH 7.5 (all Sigma). DTNB reduction was measured photometrically over time at 405 nm (Schildknecht *et al.*, 2009).

NAD^+ measurement

Cellular NAD^+ content was determined as described before. In brief, cells were lysed with 0.5 M perchloric acid on ice. After 15 min, samples were centrifuged at 1.500× *g* for 10 min at 4°C. The supernatant (500 μL) was combined with 350 μL of 1 M KOH, 0.33 M K_2HPO_4, 0.33 M KH_2PO_4 and NAD^+ was determined using an enzymic cycling assay (Weidele *et al.*, 2010).

Quantitative image analysis

Following treatment, cells were stained for the neuronal marker β-III-tubulin (using the monoclonal antibody Tuj1) or for poly-(ADP-ribose) (PAR). An Array-Scan VTI HCS Reader (Cellomics, Pittsburgh, PA, USA) equipped with a Hamamatsu ORCA-ER camera (Hamamatsu Photonics, Hamamatsu City, Japan) was used for image acquisition. Thirty fields per well (330 × 330 μm size each) were imaged in one channel using a 20× objective. Image sets were analysed using the Thermo Scientific Cellomics Spot Detector Bioapplication V4 as described earlier (Krug *et al.*, 2013). For each data point, 30 images were captured automatically and analysed by the software, as demonstrated in Supporting Information Fig. S3.

siRNA-mediated knock-down of PARP1

LUHMES were differentiated for 2 days according to the standard protocol. For transfection, solution A, consisting of 7.5 μL of Lipofectamine™ RNAiMAX (Invitrogen, Carlsbad, CA, USA) and 150 μL Opti-MEM I (Gibco, Paisley, UK), and solution B, consisting of 120 pmoles of the respective siRNA

and 150 μL Opti-MEM I, were mixed and incubated for 5 min at room temperature. Following incubation, both solutions were combined, transferred into 6-well plates and incubated for 20 min. The amounts indicated refer to one well of a 6-well plate. Next, pre-differentiated and trypsinized LUHMES cells were added in a volume of 1.7 mL DM to the siRNA containing solution at a density of 1.5×10^6 cells per well (6-well plate) and thoroughly mixed. After the additional 3 days, cells were harvested for Western blot analysis and for toxicological experiments. siRNA oligonucleotides were obtained from Sigma targeting the 3′UTR of PARP1: AACGTGTTAAAGGTTTTCTCTAA, or a randomized control sequence of the PARP1 target sequence, termed PARP1 scrambled AATCCGATGTTATTCGTGTATAA.

Data analysis

All data were confirmed in at least two (usually three) different experiments. Values are expressed as the mean ± SD ($n \geq 3$) (unless otherwise stated). Data were analysed by one-way ANOVA, two-way ANOVA or Student's *t*-test as appropriate. Differences between treatment groups in multiple comparisons were determined by Bonferroni's or Dunnett's *post hoc* test (GraphPad Software, San Diego, CA, USA).

Materials

GSSG (oxidized L-glutathione), DHQ (1,5-isoquinolinediol), rasagiline, GBR12909, deprenyl, ascorbic acid, deferoxamine, HA-1077, L-NMMA, 1400W, L-NNA, minocycline, 7-nitroindazole, MPTP and MPP^+ were obtained from Sigma (St. Louis, MO); caspase inhibitor I (zVADfmk) from Calbiochem (San Diego, CA, USA); Y-27632 was from Tocris Bioscience (Bristol, UK). CEP1347 (3,9-bis[(ethylthio) methyl]-K-252a) was obtained by chemical modification of K252a (Calbiochem, San Diego, CA) according to standard methods (Kaneko *et al.*, 1997).

The antibodies used in this study were supplied as follows: primary antibodies: monoclonal mouse anti-S-100 (ß-subunit) antibody, clone SH-B1, isotype IgG1, was used for immunocytochemistry at a dilution of 1:500 (catalog number S2532, Sigma), monoclonal mouse anti-neuronal class III β-tubulin antibody, clone TUJ1, isotype IgG2a, was used for immunocytochemistry at a dilution of 1:500 and for Western blot analysis at a dilution of 1:1000 (catalog number MMS435P, Covance); monoclonal mouse anti-GAPDH antibody, clone GAPDH-71.1, isotype IgM, was used for Western blot analysis at a dilution of 1:10 000 (catalog number G8795, Sigma); monoclonal rat anti–DAT antibody, clone DAT-Nt, isotype IgG2ak was used for immunocytochemistry at a dilution of 1:500 (catalog number MAB369, Millipore); monoclonal mouse anti-TH antibody, clone LNC1, isotype IgG1k was used for immunocytochemistry at a dilution of 1:500 and for Western blot analysis at a dilution of 1:1000 (catalog number MAB318, Millipore); rabbit anti-human VMAT2 antibody (catalog number AB1767, Chemicon) was used for immunocytochemistry at a dilution of 1:500; monoclonal mouse anti-NeuN antibody, clone A60, isotype IgG1 was used for immunocytochemistry at a dilution of 1:200 (catalog number MAB377, Millipore); monoclonal mouse anti-PAR antibody (clone 10H) and monoclonal mouse anti-PARP1 antibody (clone FI-2-3) were obtained as previously decribed (Fischer *et al.*, 2014; Kawamitsu *et al.*, 1984). They were used for both immunocytochemistry and Western blot analysis at a dilution of 1:300.

Secondary antibodies: Alexa Fluor 555 goat anti-mouse IgG2a antibody was used for immunostaining at a dilution of 1:1000 (catalog number A-21137, Life technologies); Alexa Fluor 488 goat anti-rat IgG antibody was used for immunostaining at a dilution of 1:1000 (catalog number A-11006, Life technologies); Alexa Fluor 488 chicken anti-rabbit IgG antibody was used for immunostaining at a dilution of 1:1000 (catalog number A-21441, Life technologies); Alexa Fluor 488 goat anti-mouse IGg2a antibody was used for immunostaining at a dilution of 1:1000 (catalog number A-21131, Life technologies) Alexa Fluor 488 goat anti-mouse IgG1 antibody was used for immunostaining at a dilution of 1:1000 (catalog number A-21121, Life Technologies), Alexa Fluor 555 goat anti-mouse IgG antibody was used for immunostaining at a dilution of 1:500 (catalog number A-21422, Life Technologies), peroxidase-conjuated goat anti-mouse IgG antibody was used for Western blot analysis at a dilution of 1:2000 (catalog number 115-035-174, Jackson Immuno Research.

Results

Establishment of the co-culture model

For mono-cultures of LUHMES or IMA cells (Figure 1A), usually different types of media are being used. In particular, the full differentiation of LUHMES into mature, post-mitotic DA neurons requires the presence of the differentiation factors dibutyryl–cAMP and glial-derived neurotrophic factor in a strictly defined growth medium. Pilot experiments showed that astrocytes can be maintained under these medium conditions without significant influence on their function and morphology. For the construction of co-cultures with precisely defined cell ratios, LUHMES cells were pre-differentiated for 2 days to arrest their cell cycle, before they were plated onto a dense layer of IMA in LUHMES DM. Then, the cells were allowed to differentiate further to neurons with an extended neurite network during the following 4 days. Co-cultures had an astrocyte : neuron ratio of 1.3 and were used at this stage for treatment with MPTP and pharmacological agents (Figure 1B). Cell type-specific immunostaining with anti-β-III-tubulin (LUHMES) or with anti-S100β (IMA) antibodies allowed a clear identification of both cell types, and showed that LUHMES cells were mainly layered on top of the astrocytes. Characterization of the culture morphology and composition across many separate experiments indicated that LUHMES can be reproducibly differentiated in the presence of IMA astrocytes to a phenotype similar to that obtained by differentiation of LUHMES mono-cultures (Figure 1C). The co-cultured neurons contained more tyrosine hydroxylase (TH) (Figure 1D), and had a higher dopamine content (Supporting Information Fig. S1A). Immunostaining showed that they express TH, the DAT and the vesicular monoamine transporter (Figure 1E; Supporting Information Fig. S1B).

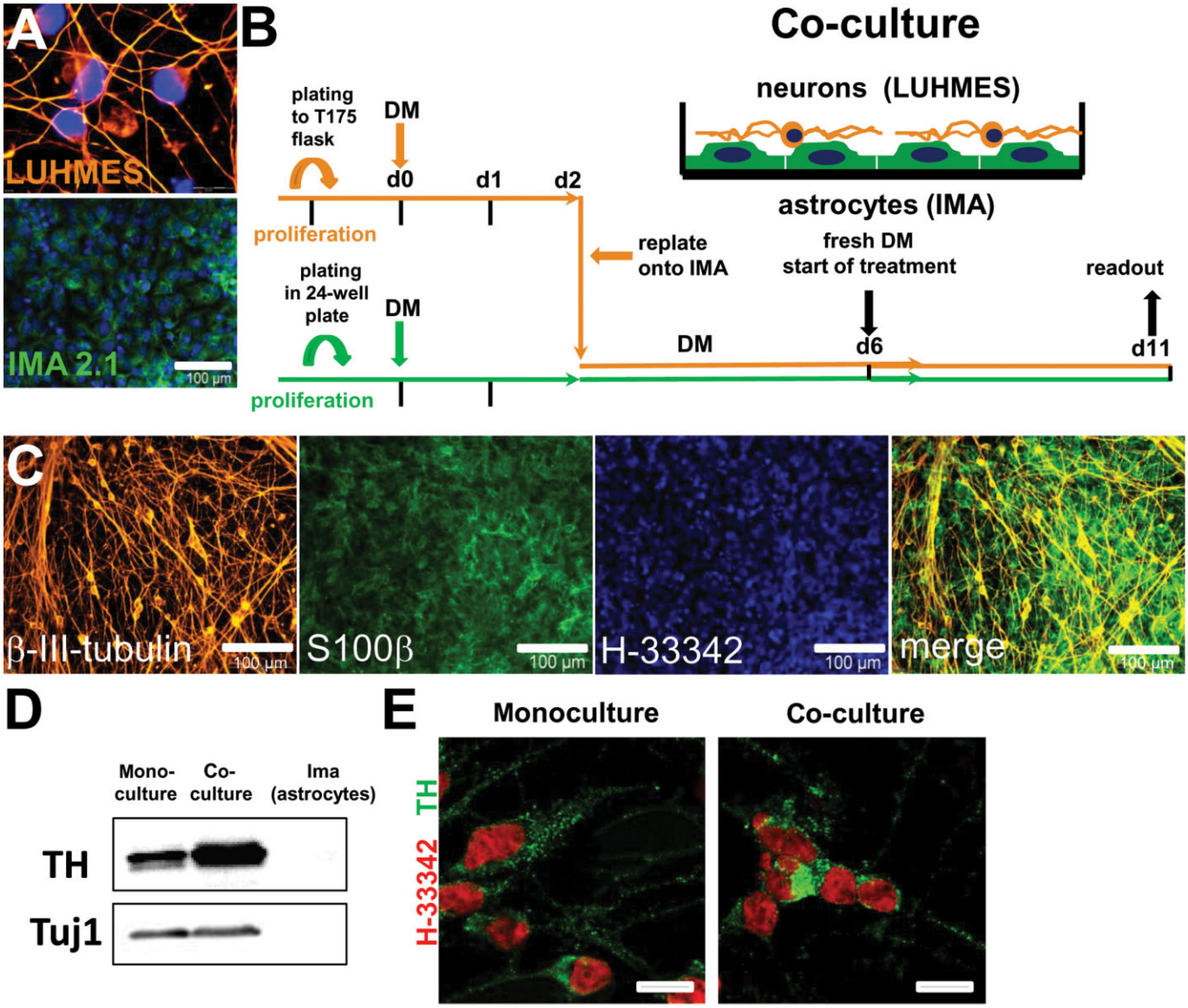

Figure 1

Schematic representation and phenotypic characterization of neuron–astrocyte co-cultures. (A) Fully differentiated LUHMES (neurons) were stained after 6 days (d6) for the neuronal-specific marker Tuj1 (β-III-tubulin) (orange). IMA 2.1 (astrocytes) were stained for the astrocyte-specific marker S100β (green). (B) Experimental procedure for generation and application of co-cultures using neurons and astrocytes. IMA were seeded in culture dishes and grown until confluence was reached. Then, LUHMES differentiation medium was added to the IMA mono-culture for 2 days. In parallel, LUHMES in mono-culture were pre-differentiated for 2 days, trypsinized, seeded on top of the IMA cultures and differentiated for additional 4 days to yield a total LUHMES differentiation period of 6 days. (C) Co-cultures of neurons and astrocytes were generated as described in panel (B), and phenotypic assessment was performed on d6 of LUHMES differentiation, by immunostaining for Tuj1 (orange) and S100β (green). Nuclei were stained with H-33342 (blue). (D) Cell lysates from mono-culture of fully differentiated LUHMES (mono), IMA mono-cultures (IMA) and co-cultures (Co) were analysed by Western blot for TH protein. The detected band was 60 kDa. The neuronal marker Tuj was analysed as loading control. (E) LUHMES cells differentiated in mono-cultures and co-cultures were stained on day 6 (d6) for TH (green). Nuclei were stained with H-33342 (red). Scale bar = 20 µm.

MPTP metabolism and toxicity in co-cultures

MPTP is a non-toxic compound and it leaves LUHMES cells unharmed (Schildknecht *et al.*, 2009), while its metabolite MPP^+ is very toxic for dopaminergic cells. We examined whether the co-culture model recapitulated the *in vivo* conversion of MPTP and subsequent neurotoxicity. We observed a time-dependent decrease of MPTP levels in the supernatant that was accompanied by the formation of MPP^+. The metabolism was completely blocked by the MAO-B inhibitor deprenyl (Figure 2A). In order to define which of the cells in the co-culture were responsible for the conversion, IMA and LUHMES mono-cultures were exposed to MPTP (30 µM) and the amount of remaining MPTP or formed metabolites ($MPDP^+$ and MPP^+) was detected by HPLC. IMA showed

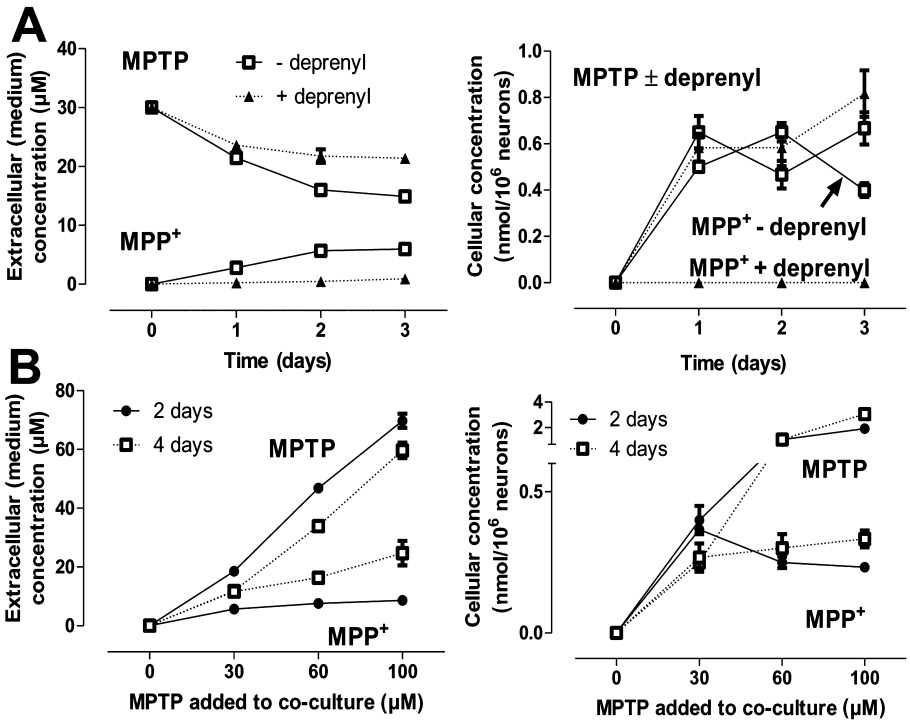

Figure 2

MPTP conversion in co-culture of LUHMES and IMA. (A) Co-cultures were treated with 30 µM MPTP in the presence or absence of the MAO-B inhibitor deprenyl (10 µM). After the periods indicated, extracellular and intracellular MPTP and MPP^+ contents were measured by HPLC. Intracellular concentrations are expressed as the amount of compound per number of neurons. Parallel experiments showed that intracellular levels of MPP^+ in IMA mono-cultures were always below the detection limit. (B) Different concentrations of MPTP were added to co-cultures. The amounts of extracellular and intracellular MPTP and MPP^+ were measured by HPLC after 2 and 4 days. Data are expressed as means ± SD of quadruplicates.

similar MPTP conversion kinetics as co-cultures, while LUHMES had no metabolizing capacity. Data obtained with the IMA cell line were fully confirmed with primary astrocytes. Thus, we assumed that all metabolic conversion of MPTP depended on the added astrocytes (Supporting Information Fig. S2).

When we examined intracellular levels of MPTP and its metabolite MPP^+ in co-cultures, it became evident that the MPP^+ concentration reached saturation levels after, at most, 24 h. MPTP concentrations of 60–100 µM did not produce higher intracellular MPP^+ levels than 30 µM MPTP, but they resulted in a higher release of extracellular MPP^+ and a higher passive diffusion of MPTP into the cells (Figure 2A,B). In this context, it is important to note that MPP^+ did not accumulate at all in IMA mono-cultures, so that it is reasonable to assume that all cellular MPP^+ measured in co-cultures was contained in LUHMES cells. This intracellular MPP^+ amount was well within the range required to evoke neurotoxicity in LUHMES mono-cultures exposed to MPP^+ (Schildknecht *et al.*, 2009). We concluded that conversion of MPTP by IMA astrocytes is sufficient to trigger degeneration of co-cultured LUHMES cells.

For specific detection of neurodegeneration in the mixed co-culture model, cells were stained for the neuronal protein β-III-tubulin. Then, the overall neuronal area was recognized and quantified by an automated and unbiased imaging algorithm on a high-content imaging system. Treatment of co-cultures with MPTP for 5 days led to a pronounced loss of neurons (Supporting Information Fig. S3A). This loss was reproducibly quantifiable with a small relative error. Toxicity was concentration dependent in the range of 0–50 µM MPTP and then reached a saturation level of about 50% (Supporting Information Fig. S3B,C). The data from IMA-LUHMES co-cultures were essentially confirmed in co-cultures of primary rat astrocytes and LUHMES (Supporting Information Fig. S4). Moreover, we counted surviving cells after staining of the culture for the neuronal nuclear marker NeuN. As we observed that neurite degeneration preceded the loss of cell somata, quantification of cell counts was performed 24 h after the quantification of the neuronal area. Under these conditions, the overall neuronal area correlated well with a manual count of remaining neuronal cell bodies (Supporting Information Fig. S5). Thus, the addition of astrocytes to human dopaminergic neurons allowed the assessment of MPTP neurotoxicity.

As a final control, we examined whether MPTP or its metabolites affected cells. They were characterized for different functional and viability parameters. Resazurin reduction, intracellular ATP and GSH levels remained at control levels. Moreover, no morphological changes were observed (Supporting Information Fig. S6A,B). We also observed no inflammatory activation when IMA were directly challenged, but

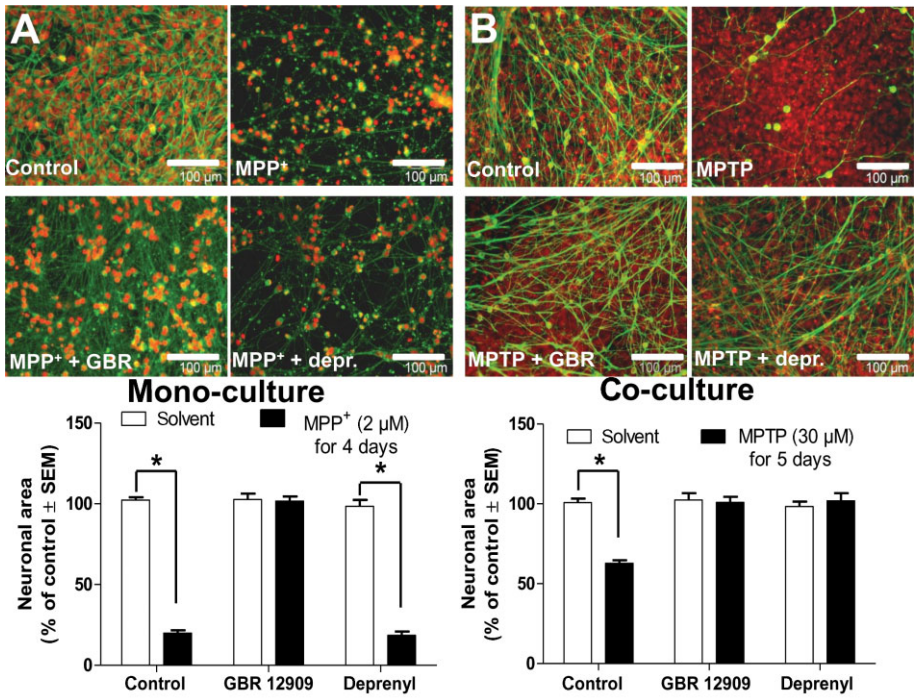

Figure 3

Differential effects of pharmacokinetic modifiers on toxicity of MPTP in co-cultures and MPP+ in mono-cultures. (A) Mono-cultures of LUHMES cells were exposed to MPP+ (2 µM) for 4 days in the presence or absence of the DAT inhibitor GBR12909 (1 µM), or the MAO-B inhibitor deprenyl (depr; 10 µM). (B) Co-cultures were exposed to 30 µM MPTP for 5 days in the presence or absence of GBR12909 (1 µM), or deprenyl (10 µM). For visualization and quantification, both mono-cultures and co-cultures were fixed, permeabilized and immunostained for the neuron-specific protein β-III-tubulin (green), nuclei were stained with Hoechst H-33342 (red). The neuronal area was quantified by an automated imaging approach. Data are means ± SEM of three different experiments.

they up-regulated, for example, IL-6, when exposed to debris from dead neurons (Supporting Information Fig. S6C,D).

Pharmacokinetic characterization of MPTP toxicity in LUHMES mono- and co-cultures

For pharmacological studies, we attempted to compare the MPTP toxicity in co-cultures with the better characterized effect of MPP+ on mono-cultures. Mono-cultures exposed to MPP+ (2 µM) for 4 days showed significant cell death (Figure 3A). For co-cultures, a standard concentration of 30 µM MPTP (for 5 days) was chosen for all following experiments (Figure 3B). For a basic characterization, the MPP+ model (mono-culture) and the MPTP model (co-culture) were compared in terms of the effects of the DAT blocker GBR12909 or the MAO-B inhibitor deprenyl (Figure 3A,B). The DAT blocker was neuroprotective in both models. This indicates formation of MPP+ from MPTP and its release into the medium in the co-culture model. The MAO-B inhibitor deprenyl completely prevented toxicity of MPTP, but not of MPP+. These data confirm that MPTP is converted by MAO-B into MPP+ in the co-culture model of LUHMES and IMA (Figure 3A,B). The results from these experiments confirm the expected metabolic and distribution behaviour known from *in vivo* experiments.

An additional finding of these experiments was that the presence of astrocytes affected neurons not only by their xenobiotic metabolism. The toxicity of MPTP co-cultures was consistently less pronounced than MPP+ toxicity in mono-cultures, also when higher MPTP concentrations were applied. The difference was not due to obviously altered neuronal morphology or numbers, and the amount of β-III-tubulin per culture well was very similar in both models. Therefore, we expected some biochemical changes, and more detailed characterization experiments showed indeed that co-cultured neurons took up less MPP+ than the same cells in mono-culture (Supporting Information Fig. S7). In subsequent experiments we examined whether the differences in the culture systems also resulted in pharmacological differences when potentially neuroprotective agents were tested.

Involvement of PARP activation in the LUHMES/MPP+ model

The damaging mechanism and pharmacological target process most consistently found in rodents exposed to MPTP, and also other PD models, is the activation of PARP (Mandir *et al.*, 1999; Lee *et al.*, 2013; 2014). The resulting formation of PAR can be readily measured on a single cell level. We examined here first whether PARP played also a role in human LUHMES neurons exposed to MPP+. In mono-cultures exposed to the toxicant, we observed the formation of PAR in the nucleus of individual neurons, and this was prevented by the PARP inhibitor 1,5-isoquinolinediol (DHQ) (Figure 4A). The drug also prevented neuronal death, as assessed by the resazurin reduction assay (Figure 4B), and Western blot analy-

Figure 4

Protection from MPP^+ toxicity in LUHMES mono-culture by PARP1 inhibition. (A) LUHMES (d6) were treated with 5 μM MPP^+ alone or in combination with the PARP inhibitor DHQ (50 μM). After 24 h, cells were fixed and immunostained for PAR, and nuclei were counterstained with H-33342. (B) LUHMES were pre-differentiated for 2 days and re-plated in the presence of 120 pmoles siRNA for additional 3 days. A siRNA against PARP1 and a scrambled siRNA (control) were used. On day 5 of differentiation, cells were treated with 5 μM MPP^+ or solvent for three additional days. The PARP inhibitor DHQ (50 μM) was used as a positive control. Viability was assessed by the resazurin reduction assay. (C) LUHMES (d6) were treated with 5 μM MPP^+ alone or in combination with 50 μM DHQ. After 24 h, cell lysates were analysed by Western blot for proteins modified by PAR. Detection was in the molecular weight range of 250–400 kDa. (D) LUHMES cells were exposed to siRNA (as in B) on day 2 of differentiation and incubated for additional 72 h. Then, cell lysates were analysed by Western blot on day 5 of LUHMES differentiation for the PARP1 protein content. Data are means ± SD of quadruplicates.

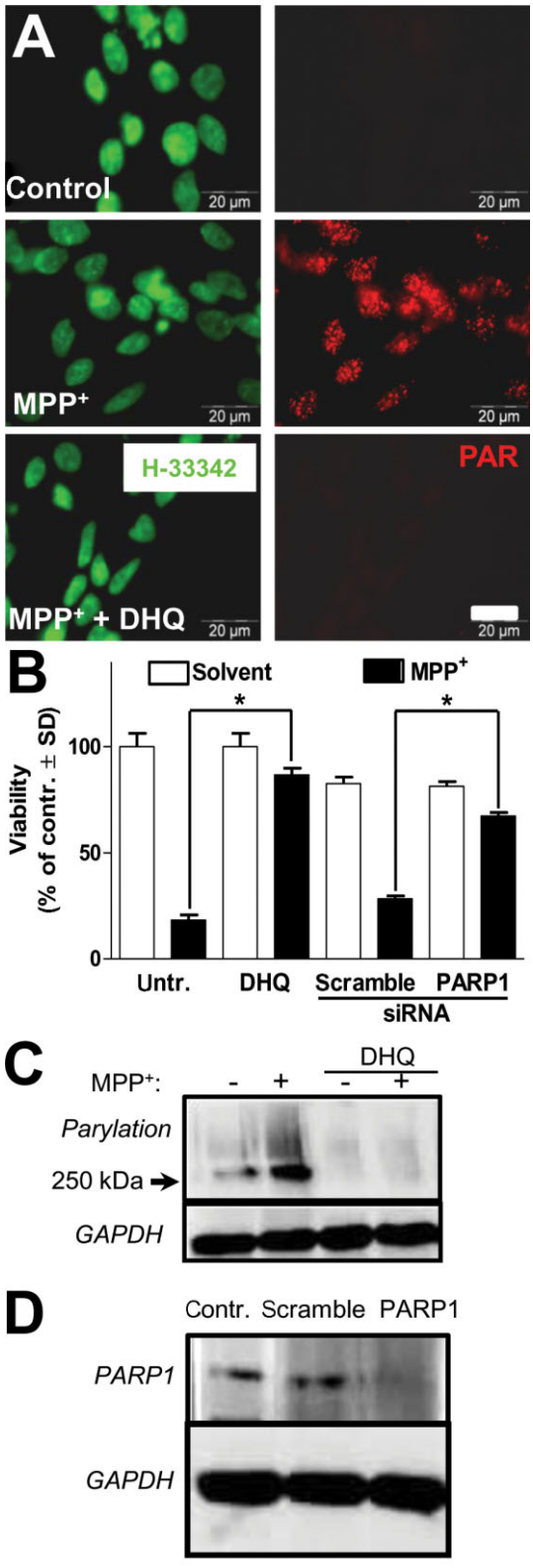

sis showed that protein PARylation was efficiently reduced (Figure 4C). The prevention of cell death by DHQ correlated well with preservation of cellular ATP and NAD^+ levels (Supporting Information Fig. S8).

We probed the role of PARP also using a siRNA selective for PARP-1. The Decreased cell death also followed this intervention (Figure 4B) and these effects correlated with a down-regulation of PARP-1 levels (Figure 4D). Thus, PARP played a role in the degeneration of human LUHMES neurons exposed to MPP^+.

Involvement of PARP activation in the LUHMES/IMA co-culture MPTP model

We observed PAR formation within neurons upon MPTP treatment, and this was blocked by the PARP inhibitor DHQ. IMA alone were not affected (Figure 5A,B). Inhibition of PARP by DHQ (at 50–200 μM) resulted in a rescue from MPTP toxicity in co-cultures (Figure 5C,D), and ABT-888, another PARP inhibitor, showed similar rescuing effects (at 10 μM). Taken together, these data show that the co-culture model shows degeneration mechanisms also known from *in vivo* models, and that it was able to identify potentially neuroprotective compounds.

Pharmacological protection in the mono- versus co-culture models

To obtain a broader range of data on the effect of drugs and experimental treatments in the co-culture MPTP model, we assembled a set of compounds to be tested. These were compared in standard mono-cultures exposed to MPP^+ (Figures 6A and 7A), and LUHMES/IMA co-cultures exposed to MPTP (Figures 6B and 7B). Viability of the neurons was assessed by morphological observation, and by high-content imaging of neurons.

LUHMES mono-cultures were protected from MPP^+ by ascorbic acid (Vit C), by the mixed lineage kinase inhibitor CEP1347 (3,9-bis[(ethylthio)methyl]-K-252a) or by the caspase/protease inhibitor zVAD. No protection was offered by the clinically used MAO inhibitor rasagiline. These data essentially corroborated our earlier observations (Poltl *et al.*, 2012). The situation was exactly reversed in the MPTP model:

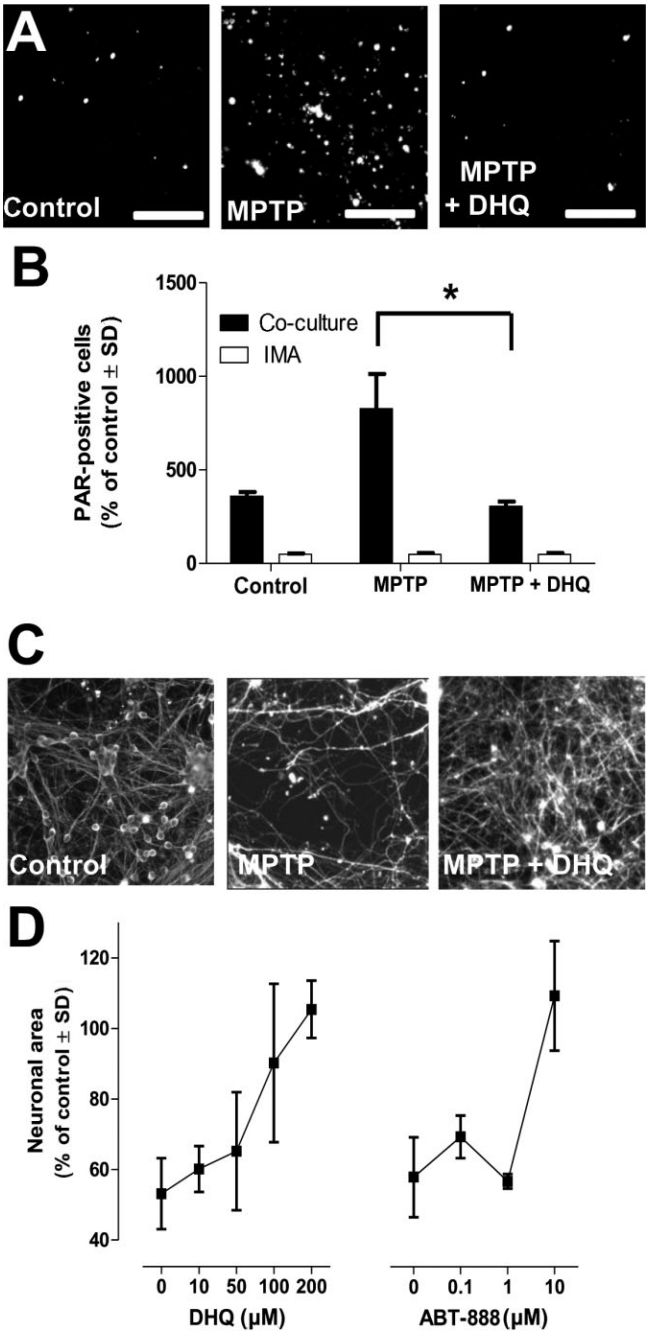

Figure 5

Neuroprotective effects of PARP inhibition in co-culture of neurons and astrocytes. (A) Co-cultures were treated with MPTP (30 μM) alone or in the presence of DHQ (200 μM) for 72 h. Then, cells were fixed and immunostained for PAR. (B) Images of co-cultures or IMA alone were additionally analysed by an automated imaging acquisition system. The algorithm applied for quantification recognizes cell nuclei stained for PAR and quantifies the number of PAR-positive cells in 30 fields per well. (C) Representative images (β-III-tubulin staining) of co-cultures exposed to MPTP (30 μM) in the presence or absence of DHQ (200 μM) for 5 days. (D) Concentration-dependent effects of the PARP inhibitors DHQ and ABT-888 on neuronal area in co-cultures exposed to MPTP (30 μM) for 5 days. Cells were stained for β-III-tubulin after treatment, and the neuronal area was analysed by an automated imaging approach. Data are presented as means ± SD.

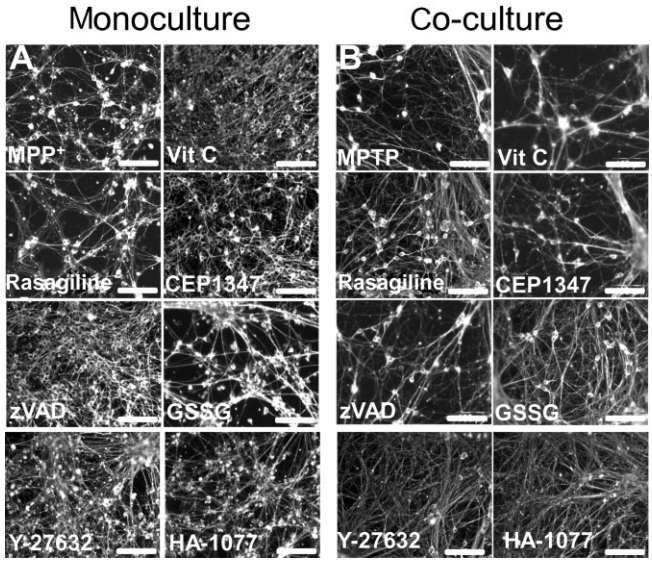

Figure 6

Profiling of neuroprotective candidate compounds in LUHMES mono-cultures and co-cultures. Mono-cultures (A) were exposed to MPP^+ (2 μM, 4 days); co-cultures (B) were exposed to MPTP (30 μM, 5 days) in the presence or absence of ascorbic acid (Vit C; 200 μM), rasagiline (Rasa; 10 μM), CEP1347 (CEP; 250 nM), zVAD-OMe-fmk (zVAD; 50 μM), GSSG (100 μM), Y-27632 (10 μM) and HA-1077 (10 μM). Cells were fixed, permeabilized and immunostained for β-III-tubulin. Representative images were displayed in b/w and without nuclear stain for optimal contrast.

CEP1347, zVAD and Vit C failed to protect from neurodegeneration. They also failed to rescue the neurons when added several times during the culture period (not shown) or when used in various combinations (Figure 8). The same differential protection (complete rescue of neurons in mono-cultures, but not at all in co-cultures) was also observed for the antioxidant iron chelator deferoxamine (Figure 8). Instead, rasagiline was fully protective in co-cultures (and not at all in mono-cultures), as expected from its effect on MPTP metabolism. These data showed that the MPTP co-culture model showed pharmacological properties that were strikingly different from the simplified model of direct addition of MPP^+ to neuron mono-cultures. The data obtained by quantification of the neuronal area were essentially confirmed for five drugs by counting of the cell somata (Supporting Information Fig. S5).

In order to explore whether preferential protection of neurons in co-cultures can be achieved by compounds that do not block MPTP metabolism, we tested GSSG (100 μM) based on the idea that this experimental treatment would affect neurons indirectly via neuron–glia metabolic interaction. Indeed, we observed complete protection in co-cultures versus no effect at all in mono-cultures (Figures 6 and 7). The effect was so far specific for GSSG, as reduced glutathione or cysteine showed no effect in either culture system. These findings provide additional evidence that the MPTP co-culture system developed here has properties different from mono-cultures of neurons, and that it allows the characterization of drug candidates on human neurons under more complex conditions than offered by such mono-cultures.

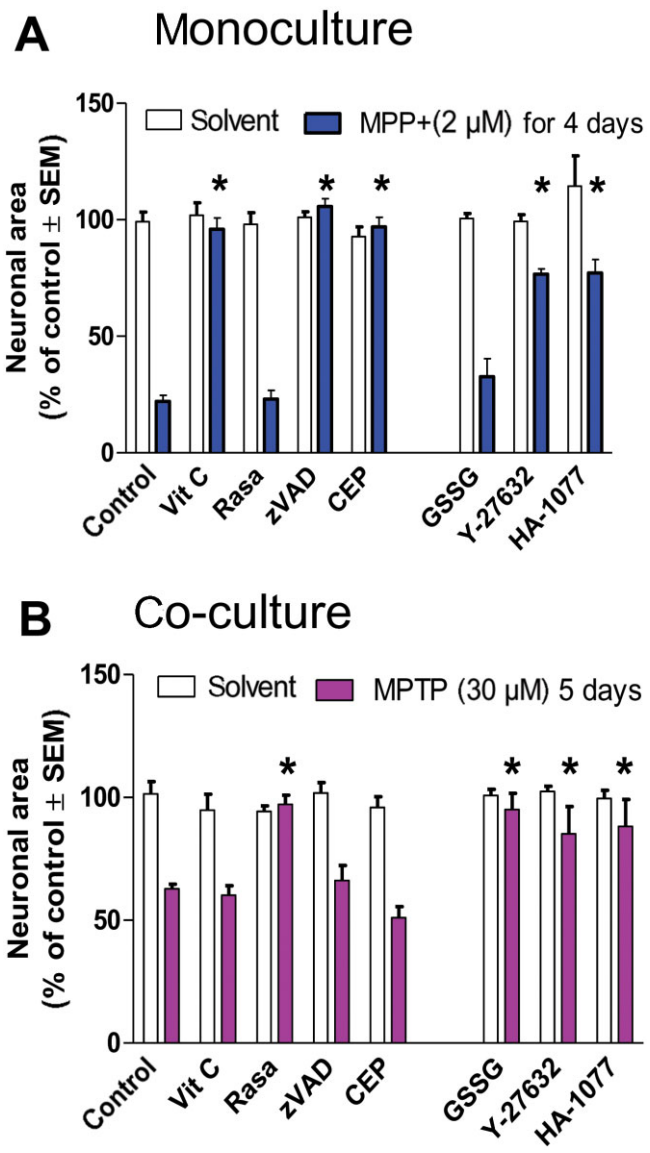

Figure 7

Quantification of neuroprotective effect of candidate compounds in LUHMES mono-cultures and co-cultures. Mono-cultures (A) and co-cultures (B) were exposed to MPP^+ or MPTP, respectively, in the presence of candidate compounds as indicated in Figure 6. Cells were stained and the total neuronal area was quantified by an automated imaging procedure. Data are presented as means ± SEM of three independent experiments. *$P < 0.05$, MPP^+ (A), MPTP (B) exposure significantly different from solvent-treated cultures.

We also evaluated the behaviour of compounds assumed to specifically protect neurites. For this purpose, the two Rho kinase (ROCK) inhibitors Y-27632 and HA-1077 were tested. We found that ROCK inhibitors protected neurons from degeneration in a concentration-dependent manner in co-culture as well as in mono-cultures (Figures 6 and 7 and Supporting Information Fig. S9). ROCK inhibitors and PARP inhibitors were the only agents we have identified so far that protected neurons when cultured alone, or together with glial cells.

As PARP activation in dopaminergic cell death has often been associated with earlier damage by peroxynitrite or other reactive nitrogen species, we explored whether this may also play a role in human LUHMES cells. Several approaches to block NO generation or to scavenge peroxynitrite failed to show any protective effect (Figure 8). Thus, PARP activation must be able to occur in human neurons independent of NO-triggered DNA damage. This may represent species differences in the regulation of NOS, and is consistent with recent discoveries on PARP activation independent of DNA damage (Lee *et al.*, 2013).

In summary, the pharmacological characterization with more than 15 compounds (Figure 8) showed that (i) the MPTP co-culture system represents a new model of degeneration of human dopaminergic neurons that reproduces key features of MPTP toxicity *in vivo* and (ii) that the pharmacological features of the more complex co-culture model are clearly distinct from those of the simple mono-culture model.

Discussion and conclusions

To our knowledge, we have presented here the first model that allows pharmacological studies of human dopaminergic neurodegeneration triggered by MPTP. The toxin has attracted a considerable amount of scientific attention, as it can induce Parkinsonian-like symptoms in young drug addicts (Langston *et al.*, 1984). The discovery that MPP^+ is the metabolite ultimately responsible for neurotoxicity has lead to the widespread use of this agent in cellular models. Such mono-culture models neither allow for the various modulatory effects of astrocytes (McNaught and Jenner, 1999; Smeyne *et al.*, 2001), nor for the considerably higher complexity of continuous toxicant production within a network of interacting cell populations. Our data provide clear evidence for major functional differences between an MPTP co-culture model, and the acute addition of MPP^+ in mono-cultures. In parallel, we show that the MPTP model reproduces essential features (drug metabolism, cellular distribution, involvement of PARP and ROCK) known from *in vivo* mouse models. The possibility to study MPTP toxicity in a co-culture model opens new ways of pharmacological tests on human neurons, and to explore many of the more recently described mechanistic pathways from animal models (Supporting Information Fig. S10).

There is a strong interest in neuroprotective compounds that prevent the degeneration of dopaminergic neurons in diseases such as PD. As all candidate drugs have failed so far in clinical trials (Olanow and Kordower, 2009; Kincses and Vecsei, 2011; Meissner *et al.*, 2011), better, more predictive drug discovery models are under high demand. One newer strategy is the use of human target cells. The availability of dopaminergic neurons generated from induced pluripotent stem cells may provide new disease models for drug testing (Sanchez-Danes *et al.*, 2012). However, such cells often show relatively immature phenotypes and are yet difficult to control for biochemical studies (Miller *et al.*, 2013). The use of LUHMES neurons that are highly committed to the dopaminergic phenotype, and that allow generation of homogeneous cultures (Scholz *et al.*, 2011), remedies some of these issues. However, pure neuronal cultures represent a rather artificial situation, as neurons in the brain are in close contact and interaction with their surrounding glial cells. Co-cultures

Compounds	Protection in monoculture	Protection in co-culture
L-NMMA *NOS inhibitor*	–	–
1400W *iNOS inhibitor*	–	–
L-NNA *nNOS, iNOS inhibitor*	–	–
Minocycline *antibiotic*	–	–
7-Nitroindazole *nNOS inhibitor*	–	–
GSSG *GSH precursor*	–	+
Deprenyl *MAO-B inhibitor*	–	+
Rasagiline *MAO-B inhibitor*	–	+
CEP 1347 *MLK inhibitor*	+	–
Ascorbic acid *antioxidant*	+	–
zVAD-OMe-fmk *caspase inhibitor*	+	–
zVAD-OMe-fmk + Ascorbic acid	+	–
CEP 1347 + Ascorbic acid	+	–
CEP 1347 + zVAD-OMe-fmk	+	–
Deferoxamine *Iron chelator*	+	–
GBR12909 *DAT inhibitor*	+	+
DHQ *PARP inhibitor*	+	+
ABT-888 *PARP inhibitor*	+	+
Y-27632 *Rock inhibitor*	+	+
HA-1077 *Rock inhibitor*	+	+

Figure 8

Comparison of potential neuroprotective compounds in LUHMES mono- and co-cultures. Mono-cultures (A) were exposed to MPP^+ (2 μM, 4 days); co-cultures (B) were exposed with MPTP (30 μM, 5 days) in the presence or absence of varying concentrations of N^G-Methyl-L-arginine acetate salt (L-NMMA; 1–1000 μM), 1400 W (0–100 μM), N_ω-Nitro-L-arginine (L-NNA, 1–500 μM), Minocycline (0–50 μM), 7-Nitroindazole (0–100 μM), GSSG (100 μM), deprenyl (10 μM), rasagiline (10 μM), CEP1347 (250 nM), ascorbic acid (200 μM), zVAD-OMe-fmk (50 μM), deferoxamine (100 μM), GBR12909 (1 μM), DHQ (50 μM in mono-culture, 200 μM in co-culture), ABT-888 (0- 200 μM), Y-27632 (10 μM) and HA-1077 (10 μM); combinations of ascorbic acid (200 μM) with zVAD-OMe-fmk (50 μM), zVAD-OMe-fmk (50 μM) with CEP1347 (250 nM) and CEP1347 (250 nM) with ascorbic acid (200 μM). Then, cells were fixed, permeabilized and immunostained for β-III-tubulin. The total neurite area was quantified by an automated imaging procedure. +, protection; –, no protection observed at any concentration.

of neurons and astrocytes may better reflect this *in vivo* situation (Allen and Barres, 2009; Sofroniew and Vinters, 2010). High-content imaging techniques addressed the additional analytical complexity of co-cultures and allowed the quantification of specific neuronal damage. The use of murine astrocytes together with the human neurons will allow for the analysis of mRNA levels by PCR in future studies, and also Western blots may be performed in a cell type-specific way if species-specific antibodies for the proteins of interest are available. Our examination of PARP inhibitors showed that mechanistic studies are possible in such co-cultures, if changes (such as PAR formation) can be imaged on the single cell level.

It would be helpful to understand why several drugs effective in the MPTP mouse model were not successful in clinical trials. A new hypothesis suggested by our findings is that the glia–neuron ratio may play a role, as this is much smaller in rodent brains than in humans (Tower and Young, 1973). Several compounds that protected neurons in mice or in mono-cultures were not effective in co-cultures (Supporting Information Fig. S11). Thus, the most striking finding of our study was the different efficacy of experimental neuroprotectants in mono-cultures versus co-cultures (Figure 8). The lack of protection in co-cultures may have several reasons: (i) some compounds might be metabolized or modified by astrocytes; (ii) the metabolic situation of neurons may be affected by astrocytes; (iii) the relative contribution of cell death mechanisms may change in the presence of astrocytes; (iv) the continuous production of MPP^+ may lead to different early stress responses and adaptations. A further explanation may apply particularly to CEP1347. At the high concentrations used here, this drug reduced intracellular GSH level in IMA mono-cultures (Supporting Information Fig. S12). This may account for the loss of neuronal protection in co-cultures, as it has been shown that astrocytes depleted of GSH are not able to protect neurons from neurotoxicants (Pizzurro *et al.*, 2014). This would be in line with a neuroprotective counter-regulatory programme triggered in LUHMES by MPP^+ (Krug *et al.*, 2014).

Three compounds that were protective in the co-culture model appear of particularly high interest to us for future more detailed characterizations.

First, we provided evidence for the lack of NO/peroxynitrite contribution in the activation of PARP. This shows, on the one hand, that PARP can be involved in human neuronal cell death, when NOS is not activated. On the other hand, these findings suggest caution concerning the human transferability of mechanisms discovered in rodents. Previous studies had suggested that generation of NO is a necessary condition for PARP overactivation, in the context of neurodegeneration (Grunewald and Beal, 1999; Mandir *et al.*, 1999). In our co-culture system, it became clear that PARP can be activated by other mechanisms, as treatment with inhibitors that completely shut down NOS activity did not show any effect.

Second, we found clear protection by two different ROCK inhibitors in mono-cultures and co-cultures. This is consistent with concepts that neuronal degeneration in PD represents a 'dying back' pathology (Burke and O'Malley, 2013), and protection of axons may prove to be beneficial (Tonges *et al.*, 2012; Chong *et al.*, 2014). The extent of protection in co-cultures was particularly striking.

Third, we identified an experimental treatment that only works in co-cultures, but not in mono-cultures, addition of GSSG. This underlines the importance of astrocyte–neuron interactions beyond simple xenobiotic metabolism, even though we cannot offer a consistent mechanistic explanation. GSSG did not increase the intracellular levels of glutathione in IMA or LUHMES mono-cultures, but we suppose that it was used by astrocytes to provide glutathione precursors to neurons. This could however not be confirmed by direct measurements, as the content of glutathione in co-cultures was not affected by GSSG addition. The depletion of glutathione as a consequence of MPTP addition was prevented by GSSG (not shown), but only complex studies of metabolite fluxes between the cell populations will show whether this effect is a direct consequence of improved GSH re-synthesis in neurons or rather secondary to other mechanisms of neuroprotection.

In summary, our study demonstrated that glial cells not only play a major role for the biology and metabolism of neurons but also drastically affect the pharmacology of neuroprotection. Moreover, our study opens the road to the construction of complex neurodegeneration models that consist of more than one cell type, but are still amenable to high throughput end points and single cell analysis of human neurons. Related systems have been used in the past mainly for the study of neuron–microglia interactions, while considerably less information is available on astrocytes (Piani *et al.*, 1992; Hirt *et al.*, 2000; Bal-Price and Brown, 2001; Kingham and Pocock, 2001; Malchiodi-Albedi *et al.*, 2001; Cacci *et al.*, 2008; Frakes *et al.*, 2014; Lee *et al.*, 2015). An important further step will be the combination of neurons, astrocytes and microglia at defined proportions, possibly also considering oligodendrocytes as a fourth type of relevant cells.

Acknowledgements

This work was supported by the Doerenkamp-Zbinden Foundation, the Land BW, the DFG (RTG1331; KoRS-CB), the BMBF and University of Konstanz funds.

Author contributions

L. E. performed the experiments and wrote the manuscript. S. S. designed the experiments and wrote the manuscript. M. A., R. P., S. G. and B. H. performed the experiments. A. B. and M. L. designed the experiments and wrote the manuscript.

Conflict of interest

The authors declare no conflict of interest.

References

Alexander SPH, Benson HE, Faccenda E, Pawson AJ, Sharman JL, Spedding M *et al.* (2013a). The Concise Guide to PHARMACOLOGY 2013/14: Transporters. Br J Pharmacol 170: 1706–1796.

Alexander SPH, Benson HE, Faccenda E, Pawson AJ, Sharman JL, Spedding M *et al.* (2013b). The Concise Guide to PHARMACOLOGY 2013/14: Enzymes. Br J Pharmacol 170: 1797–1867.

Allen NJ, Barres BA (2009). Neuroscience: glia – more than just brain glue. Nature 457: 675–677.

Bal-Price A, Brown GC (2001). Inflammatory neurodegeneration mediated by nitric oxide from activated glia-inhibiting neuronal respiration, causing glutamate release and excitotoxicity. J Neurosci 21: 6480–6491.

Burke RE, O'Malley K (2013). Axon degeneration in Parkinson's disease. Exp Neurol 246: 72–83.

Cacci E, Ajmone-Cat MA, Anelli T, Biagioni S, Minghetti L (2008). In vitro neuronal and glial differentiation from embryonic or adult neural precursor cells are differently affected by chronic or acute activation of microglia. Glia 56: 412–425.

Caudle WM, Guillot TS, Lazo CR, Miller GW (2012). Industrial toxicants and Parkinson's disease. Neurotoxicology 33: 178–188.

Chong CM, Shen M, Zhou ZY, Pan P, Hoi PM, Li S *et al.* (2014). Discovery of a benzofuran derivative (MBPTA) as a novel ROCK inhibitor that protects against MPP(+)-induced oxidative stress and cell death in SH-SY5Y cells. Free Radic Biol Med 74: 283–293.

Dauer W, Przedborski S (2003). Parkinson's disease: mechanisms and models. Neuron 39: 889–909.

Falsig J, Latta M, Leist M (2004a). Defined inflammatory states in astrocyte cultures: correlation with susceptibility towards CD95-driven apoptosis. J Neurochem 88: 181–193.

Falsig J, Porzgen P, Lotharius J, Leist M (2004b). Specific modulation of astrocyte inflammation by inhibition of mixed lineage kinases with CEP-1347. J Immunol 173: 2762–2770.

Fischer JM, Popp O, Gebhard D, Veith S, Fischbach A, Beneke S *et al.* (2014). Poly(ADP-ribose)-mediated interplay of XPA and PARP1 leads to reciprocal regulation of protein function. FEBS J 281**:** 3625–3641.

Frakes AE, Ferraiuolo L, Haidet-Phillips AM, Schmelzer L, Braun L, Miranda CJ *et al.* (2014). Microglia induce motor neuron death via the classical NF-kappaB pathway in amyotrophic lateral sclerosis. Neuron 81: 1009–1023.

Giordano G, Costa LG (2012). Morphological assessment of neurite outgrowth in hippocampal neuron-astrocyte co-cultures. Curr Protoc Toxicol 11: Unit 11.16.

Grunewald T, Beal MF (1999). NOS knockouts and neuroprotection. Nat Med 5: 1354–1355.

Hirt UA, Gantner F, Leist M (2000). Phagocytosis of nonapoptotic cells dying by caspase-independent mechanisms. J Immunol 164: 6520–6529.

Kaneko M, Saito Y, Saito H, Matsumoto T, Matsuda Y, Vaught JL *et al.* (1997). Neurotrophic 3,9-bis[(alkylthio)methyl]-and-bis(alkoxymethyl)-K-252a derivatives. J Med Chem 40: 1863–1869.

Kawamitsu H, Hoshino H, Okada H, Miwa M, Momoi H, Sugimura T (1984). Monoclonal antibodies to poly(adenosine diphosphate ribose) recognize different structures. Biochemistry 23: 3771–3777.

Kincses ZT, Vecsei L (2011). Pharmacological therapy in Parkinson's disease: focus on neuroprotection. CNS Neurosci Ther 17: 345–367.

Kingham PJ, Pocock JM (2001). Microglial secreted cathepsin B induces neuronal apoptosis. J Neurochem 76: 1475–1484.

Krug AK, Balmer NV, Matt F, Schonenberger F, Merhof D, Leist M (2013). Evaluation of a human neurite growth assay as specific screen for developmental neurotoxicants. Arch Toxicol 87: 2215–2231.

Krug AK, Gutbier S, Zhao L, Poltl D, Kullmann C, Ivanova V *et al.* (2014). Transcriptional and metabolic adaptation of human neurons to the mitochondrial toxicant MPP. Cell Death Dis 5: e1222.

Langston JW, Langston EB, Irwin I (1984). MPTP-induced parkinsonism in human and non-human primates – clinical and experimental aspects. Acta Neurol Scand Suppl 100: 49–54.

Lee M, McGeer E, McGeer PL (2015). Activated human microglia stimulate neuroblastoma cells to upregulate production of beta amyloid protein and tau: implications for Alzheimer's disease pathogenesis. Neurobiol Aging 36: 42–52.

Lee Y, Karuppagounder SS, Shin JH, Lee YI, Ko HS, Swing D *et al.* (2013). Parthanatos mediates AIMP2-activated age-dependent dopaminergic neuronal loss. Nat Neurosci 16: 1392–1400.

Lee Y, Kang HC, Lee BD, Lee YI, Kim YP, Shin JH (2014). Poly (ADP-ribose) in the pathogenesis of Parkinson's disease. BMB Rep 47: 424–432.

Leist M, Volbracht C, Fava E, Nicotera P (1998). 1-Methyl-4-phenylpyridinium induces autocrine excitotoxicity, protease activation, and neuronal apoptosis. Mol Pharmacol 54: 789–801.

Liu S, Tian Z, Yin F, Zhao Q, Fan M (2009). Generation of dopaminergic neurons from human fetal mesencephalic progenitors after co-culture with striatal-conditioned media and exposure to lowered oxygen. Brain Res Bull 80: 62–68.

Lotharius J, Falsig J, van Beek J, Payne S, Dringen R, Brundin P *et al.* (2005). Progressive degeneration of human mesencephalic neuron-derived cells triggered by dopamine-dependent oxidative stress is dependent on the mixed-lineage kinase pathway. J Neurosci 25: 6329–6342.

Malchiodi-Albedi F, Domenici MR, Paradisi S, Bernardo A, Ajmone-Cat MA, Minghetti L (2001). Astrocytes contribute to neuronal impairment in beta A toxicity increasing apoptosis in rat hippocampal neurons. Glia 34: 68–72.

Mandir AS, Przedborski S, Jackson-Lewis V, Wang ZQ, Simbulan-Rosenthal CM, Smulson ME *et al.* (1999). Poly(ADP-ribose) polymerase activation mediates 1-methyl-4-phenyl-1, 2,3,6-tetrahydropyridine (MPTP)-induced parkinsonism. Proc Natl Acad Sci U S A 96: 5774–5779.

Maroney AC, Finn JP, Bozyczko-Coyne D, O'Kane TM, Neff NT, Tolkovsky AM *et al.* (1999). CEP-1347 (KT7515), an inhibitor of JNK activation, rescues sympathetic neurons and neuronally differentiated PC12 cells from death evoked by three distinct insults. J Neurochem 73: 1901–1912.

McGeer PL, McGeer EG (2008). Glial reactions in Parkinson's disease. Mov Disord 23: 474–483.

McNaught KS, Jenner P (1999). Altered glial function causes neuronal death and increases neuronal susceptibility to 1-methyl-4-phenylpyridinium- and 6-hydroxydopamine-induced / toxicity in astrocytic ventral mesencephalic co-cultures. J Neurochem 73: 2469–2476.

Meissner WG, Frasier M, Gasser T, Goetz CG, Lozano A, Piccini P *et al.* (2011). Priorities in Parkinson's disease research. Nat Rev Drug Discov 10: 377–393.

Miller JD, Ganat YM, Kishinevsky S, Bowman RL, Liu B, Tu EY *et al.* (2013). Human iPSC-based modeling of late-onset disease via progerin-induced aging. Cell Stem Cell 13: 691–705.

Morizane A, Darsalia V, Guloglu MO, Hjalt T, Carta M, Li JY *et al.* (2010). A simple method for large-scale generation of dopamine neurons from human embryonic stem cells. J Neurosci Res 88: 3467–3478.

Olanow CW, Kordower JH (2009). Modeling Parkinson's disease. Ann Neurol 66: 432–436.

Pan-Montojo F, Schwarz M, Winkler C, Arnhold M, O'Sullivan GA, Pal A *et al.* (2012). Environmental toxins trigger PD-like progression via increased alpha-synuclein release from enteric neurons in mice. Sci Rep 2: 898.

Parkinson Study Group PI (2007). Mixed lineage kinase inhibitor CEP-1347 fails to delay disability in early Parkinson disease. Neurology 69: 1480–1490.

Pawson AJ, Sharman JL, Benson HE, Faccenda E, Alexander SP, Buneman OP *et al.*; NC-IUPHAR (2014). The IUPHAR/BPS Guide to PHARMACOLOGY: an expert-driven knowledge base of drug targets and their ligands. Nucl Acids Res 42 (Database Issue): D1098–1106.

Peng J, Liu Q, Rao MS, Zeng X (2013). Using human pluripotent stem cell-derived dopaminergic neurons to evaluate candidate Parkinson's disease therapeutic agents in MPP+ and rotenone models. J Biomol Screen 18: 522–533.

Perrier AL, Tabar V, Barberi T, Rubio ME, Bruses J, Topf N *et al.* (2004). Derivation of midbrain dopamine neurons from human embryonic stem cells. Proc Natl Acad Sci U S A 101: 12543–12548.

Piani D, Spranger M, Frei K, Schaffner A, Fontana A (1992). Macrophage-induced cytotoxicity of N-methyl-D-aspartate receptor positive neurons involves excitatory amino acids rather than reactive oxygen intermediates and cytokines. Eur J Immunol 22: 2429–2436.

Pizzurro DM, Dao K, Costa LG (2014). Astrocytes protect against diazinon- and diazoxon-induced inhibition of neurite outgrowth by regulating neuronal glutathione. Toxicology 318: 59–68.

Poltl D, Schildknecht S, Karreman C, Leist M (2012). Uncoupling of ATP-depletion and cell death in human dopaminergic neurons. Neurotoxicology 33: 769–779.

Reinhardt P, Glatza M, Hemmer K, Tsytsyura Y, Thiel CS, Hoing S *et al.* (2013). Derivation and expansion using only small molecules of human neural progenitors for neurodegenerative disease modeling. PLoS ONE 8: e59252.

Sanchez-Danes A, Richaud-Patin Y, Carballo-Carbajal I, Jimenez-Delgado S, Caig C, Mora S *et al.* (2012). Disease-specific phenotypes in dopamine neurons from human iPS-based models of genetic and sporadic Parkinson's disease. EMBO Mol Med 4: 380–395.

Schapira A, Bate G, Kirkpatrick P (2005). Rasagiline. Nat Rev Drug Discov 4: 625–626.

Schildknecht S, Poltl D, Nagel DM, Matt F, Scholz D, Lotharius J *et al.* (2009). Requirement of a dopaminergic neuronal phenotype for toxicity of low concentrations of 1-methyl-4-phenylpyridinium to human cells. Toxicol Appl Pharmacol 241: 23–35.

Schildknecht S, Kirner S, Henn A, Gasparic K, Pape R, Efremova L *et al.* (2012). Characterization of mouse cell line IMA 2.1 as a potential model system to study astrocyte functions. ALTEX 29: 261–274.

Schildknecht S, Karreman C, Poltl D, Efremova L, Kullmann C, Gutbier S *et al.* (2013). Generation of genetically-modified human differentiated cells for toxicological tests and the study of neurodegenerative diseases. ALTEX 30: 427–444.

Scholz D, Poltl D, Genewsky A, Weng M, Waldmann T, Schildknecht S *et al.* (2011). Rapid, complete and large-scale generation of post-mitotic neurons from the human LUHMES cell line. J Neurochem 119: 957–971.

Schule B, Pera RA, Langston JW (2009). Can cellular models revolutionize drug discovery in Parkinson's disease? Biochim Biophys Acta 1792: 1043–1051.

Schulz JB, Matthews RT, Muqit MM, Browne SE, Beal MF (1995). Inhibition of neuronal nitric oxide synthase by 7-nitroindazole protects against MPTP-induced neurotoxicity in mice. J Neurochem 64: 936–939.

Schulz TC, Noggle SA, Palmarini GM, Weiler DA, Lyons IG, Pensa KA *et al.* (2004). Differentiation of human embryonic stem cells to dopaminergic neurons in serum-free suspension culture. Stem Cells 22: 1218–1238.

Smeyne M, Goloubeva O, Smeyne RJ (2001). Strain-dependent susceptibility to MPTP and MPP(+)-induced parkinsonism is determined by glia. Glia 34: 73–80.

Sofroniew MV, Vinters HV (2010). Astrocytes: biology and pathology. Acta Neuropathol 119: 7–35.

Sun X, Liu J, Crary JF, Malagelada C, Sulzer D, Greene LA *et al.* (2013). ATF4 protects against neuronal death in cellular Parkinson's disease models by maintaining levels of parkin. J Neurosci 33: 2398–2407.

Tonges L, Frank T, Tatenhorst L, Saal KA, Koch JC, Szego EM *et al.* (2012). Inhibition of rho kinase enhances survival of dopaminergic neurons and attenuates axonal loss in a mouse model of Parkinson's disease. Brain 135: 3355–3370.

Tower DB, Young OM (1973). The activities of butyrylcholinesterase and carbonic anhydrase, the rate of anaerobic glycolysis, and the question of a constant density of glial cells in cerebral cortices of various mammalian species from mouse to whale. J Neurochem 20: 269–278.

Volbracht C, Leist M, Nicotera P (1999). ATP controls neuronal apoptosis triggered by microtubule breakdown or potassium deprivation. Mol Med 5: 477–489.

Weidele K, Kunzmann A, Schmitz M, Beneke S, Burkle A (2010). Ex vivo supplementation with nicotinic acid enhances cellular poly(ADP-ribosyl)ation and improves cell viability in human peripheral blood mononuclear cells. Biochem Pharmacol 80: 1103–1112.

Yacoubian TA, Standaert DG (2009). Targets for neuroprotection in Parkinson's disease. Biochim Biophys Acta 1792: 676–687.

Youdim MB (2010). Why do we need multifunctional neuroprotective and neurorestorative drugs for Parkinson's and Alzheimer's diseases as disease modifying agents. Exp Neurobiol 19: 1–14.

Zeng X, Chen J, Deng X, Liu Y, Rao MS, Cadet JL *et al.* (2006). An in vitro model of human dopaminergic neurons derived from embryonic stem cells: MPP+ toxicity and GDNF neuroprotection. Neuropsychopharmacology 31: 2708–2715.

Zhang Y, Pak C, Han Y, Ahlenius H, Zhang Z, Chanda S *et al.* (2013). Rapid single-step induction of functional neurons from human pluripotent stem cells. Neuron 78: 785–798.

Zhao X, Zhai S, An MS, Wang YH, Yang YF, Ge HQ *et al.* (2013). Neuroprotective effects of protocatechuic aldehyde against neurotoxin-induced cellular and animal models of Parkinson's disease. PLoS ONE 8: e78220.

Zimmer B, Kuegler PB, Baudis B, Genewsky A, Tanavde V, Koh W *et al.* (2011). Coordinated waves of gene expression during neuronal differentiation of embryonic stem cells as basis for novel approaches to developmental neurotoxicity testing. Cell Death Differ 18: 383–395.

Supporting information

Additional Supporting Information may be found in the online version of this article at the publisher's web-site:

http://dx.doi.org/10.1111/bph.13193

Figure S1 Dopaminergic characteristics of LUHMES differentiated in mono-culture and in co-culture with astrocytes.
Figure S2 MPTP metabolism by LUHMES, IMA 2.1 and primary glial cells.
Figure S3 Quantification of neuronal area in co-culture.
Figure S4 MPTP toxicity in co-cultures of LUHMES neurons and primary rat glial cells.
Figure S5 Comparison of drug effects on neuronal area and on the number of cell bodies.
Figure S6 Toxicity of MPTP or MPP^+ in IMA 2.1 mono-cultures.
Figure S7 Uptake of MPP^+ by LUHMES mono- and co-cultures.
Figure S8 Involvement of PARP in MPP^+-mediate LUHMES toxicity.
Figure S9 ROCK inhibition protects LUHMES mono- and co-cultures from MPP^+/MPTP toxicity.
Figure S10 Recent findings on MPTP animal models in relation to our co-culture model.
Figure S11 Synopsis of drug effects *in vivo* (animals), in humans and in co-cultures.
Figure S12 Toxicity of candidate compounds used in IMA mono-cultures.
Methods S1 Details of experimental procedures.